# Syntheses, Spectroscopic Properties, and Computational Study of (E,Z)-Ethenyl and Ethynyl-Linked BODIPYs

Published as part of The Journal of Physical Chemistry virtual special issue "William M. Jackson Festschrift".

Guanyu Zhang, Ning Zhao, Petia Bobadova-Parvanova, Maodie Wang, Frank R. Fronczek, Kevin M. Smith, and M. Graca H. Vicente\*, on

Supporting Information

**ABSTRACT:** A series of (E,Z)-ethenyl- and ethynyl-linked boron dipyrromethene (BODIPY) dimers were synthesized in 23-34% yields by condensation of pyrroles with the corresponding bis-benzaldehydes, followed by oxidation and boron complexation. The BODIPY dimers were characterized by 1H, 13C, and 11B NMR spectroscopy, highresolution mass spectrometry, and, in the cases of 1b, 2, and 3, by X-ray crystallography. The spectroscopic properties for this series of dimers were investigated in tetrahydrofuran solutions, and very similar absorption and emission profiles were observed for all dimers. Density functional theory calculations show minimal conjugation between the



two BODIPY units in the dimers, as a result of the large dihedral angle between the BODIPYs and the linker. The (E)-ethenyllinked dimer 1a showed the highest fluorescence quantum yield of all dimers investigated in this study.

#### 1. INTRODUCTION

Because of their attractive photophysical properties that include large extinction coefficients, high fluorescence quantum yields, intrinsic high photochemical stability, and structure tunability, boron dipyrromethene (BODIPY) dyes have been intensely investigated, since they were first reported 50 years ago. 1-7 Specially functionalized BODIPYs with various properties are finding important roles in both classical and newly emerging application fields, such as laser dyes, chemical sensors, <sup>9-15</sup> fluorescent switches, <sup>16-20</sup> photovoltaics/ optoelectronics, <sup>21,22</sup> photosensitizers, <sup>23-27</sup> and as fluorescent labeling agents.

In particular, the synthesis and investigation of BODIPY dimers or bis-BODIPYs has emerged as a hot research field in exploitation of improved or special photophysical properties. 36-41 Depending on the type of linker and the molecular design, these BODIPY derivatives have been shown to be good candidates as near-IR or solid-state fluorescent emitters, 42-46 energy transfer cassettes, 47-49 single oxygen generators, 50-52 light-harvesting complexes, 53 and in dye-sensitized solar cells. 54 Recently, our group has reported a series of symmetrical and unsymmetrical  $\alpha - \alpha$  C(sp<sup>3</sup>)-linked dimeric BODIPYs with serendipitous enhanced fluorescence quantum yield and larger Stokes shifts compared with monomeric BODIPYs. 55

Among the various dimeric structures, ethenyl-linked fluorophores, such as porphyrin dimers, have attracted much attention especially on the alternation of the spatial configuration and stacking mode of the molecules between the E and Z isomers.  $^{56-58}$  In 2007, Cabrera et al. reported the first (E)-ethenyl-linked BODIPY dimer through a homometathesis reaction of the corresponding 8-phenylvinyl-BODIPY monomers (Scheme 1, (i)). 59 Bröring et al. further developed a series of ethenyl- and ethynyl-linked BODIPYs via the lpha or etapyrrolic positions of the BODIPY core (Scheme 1, (ii)). However, the synthesis of a (Z)-ethenyl-linked BODIPY dimer has not yet been described, thus hampering the comparative investigation of the structures and photophysical properties of the two isomers. In addition, the methodology previously reported for the synthesis of (E)-BODIPY dimers from monomers, via metal-mediated metathesis reactions, is not applicable for the synthesis of (Z)-BODIPY dimers due to the special requirement of a Z-selective metathesis catalyst. An alternative synthetic route that involves the installation of the required stereochemistry in the linker first, rather than from direct coupling of monomers, is more versatile. Herein, we describe the facile synthesis of (E)- and (Z)-ethenyl-linked BODIPY dimers from the corresponding bis-benzaldehyde cores to the BODIPY branches. This methodology takes advantage from the well-established stereoselective syntheses of (E)- and (Z)-4,4'-formylstilbene, <sup>61,65</sup> followed by the classical BODIPY formation involving pyrrole condensation, oxidation, and boron complexation. To further explore the role of the linker, an ethynyl-linked BODIPY dimer was also prepared from 4,4'-(ethyne-1,2-diyl)dibenzaldehyde. A system-

Received: May 30, 2018 Revised: July 2, 2018 Published: July 4, 2018



<sup>&</sup>lt;sup>†</sup>Department of Chemistry, Louisiana State University, Baton Rouge, Louisiana 70803, United States

<sup>\*</sup>Department of Chemistry, Rockhurst University, Kansas City, Missouri 64110, United States

Scheme 1. Approaches to (E,Z)-Ethenyl-Linked BODIPYs

atic comparison of all dimers with a BODIPY monomer was conducted to evaluate the influence of linker on their spectroscopic and photophysical properties.

# 2. EXPERIMENTAL SECTION

**2.1. Synthesis.** 2.1.1. Materials. Commercially available chemical reagents and solvents were used without further purification. Reactions were monitored by thin-layer chromatography (TLC) on precoated silica gel plates (polyester backed, 60 Å, 0.2 mm). Purifications were performed by column chromatography on silica gel (230-400 mesh, 60 Å) and by preparative TLC. 1H, 11B, and 13C NMR spectra were measured on NMR spectrometers (400 or 500 MHz for <sup>1</sup>H NMR, 100 or 125 MHz for <sup>13</sup>C NMR, and 128 MHz for <sup>11</sup>B NMR using tetramethylsilane (TMS) or BF3·OEt2 as external reference) at 300 K. Chemical shifts ( $\delta$ ) are given in parts per million (deuterated chloroform at 7.27 ppm for <sup>1</sup>H NMR and 77.0 ppm for <sup>13</sup>C NMR) relative to TMS. High-resolution mass spectra (HRMS) were obtained in the electrospray ionization time-of-flight (ESI-TOF) mode. Data utilized to determine the crystal structures were collected at low temperature on a Bruker Kappa Apex-II DUO diffractometer equipped with a focusing monochromator for the Mo X-ray beam, a Cu microfocus X-ray source, and a sample chiller.

2.1.2. General Procedure for Preparing BODIPY Dimers. To a stirred solution of dialdehyde (47 mg, 0.20 mmol) and 2-ethoxycarbonyl-3,4-dimethylpyrrole (133 mg, 0.80 mmol) $^{62}$  in dichloromethane (10 mL) was added three drops of BF<sub>3</sub>·OEt<sub>2</sub>

under an argon atmosphere. After the solution was stirred for 24 h at room temperature, 2,3-dichloro-5,6-dicyano-1,4-benzoquinone (DDQ; 91 mg, 0.40 mmol) in dichloromethane (3 mL) was added to the mixture. The reaction mixture was stirred for another 1 h, and triethylamine (0.6 mL) and BF<sub>3</sub>· OEt<sub>2</sub> (0.6 mL) were quickly added to the mixture under ice bath. The reaction was allowed to warm to room temperature and was continually stirred for 8 h, until TLC indicated disappearance of dialdehyde. The mixture was washed with 1 M HCl (1 × 20 mL), saturated NaHCO<sub>3</sub> (1 × 20 mL), and saturated NaCl (1 × 20 mL) before it was dried over anhydrous Na<sub>2</sub>SO<sub>4</sub>. The solvent was removed under vacuum, and the residue was purified by silica gel column chromatography (elution: hexanes/ethyl acetate 3:1).

(*E*)-Ethenyl-BODIPY Dimer 1a. This BODIPY was prepared from (*E*)-4,4′-formylstilbene<sup>65</sup> and 2,4-dimethyl-1*H*-pyrrole-3-carboxylic acid ethyl ester, yielding 59 mg (31%) of the dimer as a red solid. mp (°C) > 202 decomp; <sup>1</sup>H NMR (400 MHz, CDCl<sub>3</sub>) δ 7.74 (d, J = 8.1 Hz, 4H), 7.32 (s, 2H), 7.29 (d, J = 8.1 Hz, 4H), 4.47 (q, J = 7.1 Hz, 8H), 2.01 (s, 12H), 1.44 (t, J = 7.1 Hz, 12H), 1.40 (s, 12H); <sup>13</sup>C NMR (126 MHz, CDCl<sub>3</sub>) δ 162.20, 147.80, 145.32, 141.89, 138.24, 134.31, 133.13, 129.53, 129.17, 128.20, 127.68, 62.00, 14.01, 12.42, 9.56; <sup>11</sup>B NMR (CDCl<sub>3</sub>, 128 MHz) δ 0.24 (t, J = 27.6 Hz); HRMS (ESI-TOF) m/z [M + K]<sup>+</sup> 999.3725 calcd for  $C_{52}H_{54}B_2F_4KN_4O_8$  999.3712.

(*E*)-Ethenyl-BODIPY Dimer 1b. This BODIPY was prepared from (*E*)-4,4'-formylstilbene<sup>65</sup> and 4-ethyl-2-methyl-1*H*-pyrrole-3-carboxylic acid ethyl ester, yielding 69 mg (34%) of the dimer as a red solid. mp (°C) > 215 decomp; <sup>1</sup>H NMR (400 MHz, CDCl<sub>3</sub>) δ 7.75 (d, *J* = 8.2 Hz, 4H), 7.33 (s, 2H), 7.32 (d, *J* = 7.3 Hz, 4H), 4.47 (q, *J* = 7.1 Hz, 8H), 2.45 (q, *J* = 7.4 Hz, 8H), 1.50–1.35 (m, 24H), 1.04 (t, *J* = 7.5 Hz, 12H); <sup>13</sup>C NMR (126 MHz, CDCl<sub>3</sub>) δ 162.27, 147.77, 145.20, 141.33, 138.21, 135.55, 134.36, 133.13, 129.16, 128.19, 127.69, 62.00, 17.52, 14.69, 13.98, 12.12; <sup>11</sup>B NMR (128 MHz, CDCl<sub>3</sub>) δ 0.23 (t, *J* = 28 Hz); HRMS (ESI-TOF) m/z [M + Na]<sup>+</sup> 1039.4606 calcd for C<sub>56</sub>H<sub>62</sub>B<sub>2</sub>F<sub>4</sub>N<sub>4</sub>NaO<sub>8</sub> 1039.4582.

(*Z*)-Ethenyl-BODIPY Dimer **2**. This BODIPY was prepared from (*Z*)-4,4'-formylstilbene, <sup>61</sup> yielding 44 mg (23%) of the dimer as a red solid. mp (°C) > 184 decomp; <sup>1</sup>H NMR (CDCl<sub>3</sub>, 400 MHz)  $\delta$  7.38 (d, J = 8.1 Hz, 4H), 7.12 (d, J = 8.1 Hz, 4H), 6.85 (s, 2H), 4.45 (q, J = 7.1 Hz, 8H), 1.99 (s, 12H), 1.42 (t, J = 7.1 Hz, 12H), 1.39 (s, 12H); <sup>13</sup>C NMR (CDCl<sub>3</sub>, 125 MHz)  $\delta$  162.14, 147.65, 145.34, 141.59, 138.54, 133.72, 133.04, 130.96, 130.19, 129.60, 127.65, 62.00, 13.99, 12.34, 9.58; <sup>11</sup>B NMR (CDCl<sub>3</sub>, 128 MHz)  $\delta$  0.20 (t, J = 27.6 Hz); HRMS (ESI-TOF) m/z [M + H]<sup>+</sup> 961.4166 calcd for  $C_{52}H_{55}B_2F_4N_4O_8$  961.4142.

Ethynyl-BODIPY Dimer **3** and Its Byproduct **4**. BODIPY 3 was prepared from 4,4′-(ethyne-1,2-diyl)dibenzaldehyde, <sup>63</sup> yielding 53 mg (28%) of the dimer as a red solid. mp (°C) > 220 decomp; <sup>1</sup>H NMR (CDCl<sub>3</sub>, 400 MHz)  $\delta$  7.76 (d, J = 8.2 Hz, 4H), 7.31 (d, J = 8.2 Hz, 4H), 4.47 (q, J = 7.1 Hz, 8H), 2.01 (s, 12H), 1.44 (t, J = 7.1 Hz, 12H), 1.39 (s, 12H); <sup>13</sup>C NMR (CDCl<sub>3</sub>, 125 MHz)  $\delta$  162.13, 147.03, 145.55, 141.80, 135.05, 132.90, 132.77, 129.64, 127.98, 124.36, 90.24, 62.04, 14.00, 12.46, 9.55; <sup>11</sup>B NMR (CDCl<sub>3</sub>, 128 MHz)  $\delta$  0.22 (t, J = 27.5 Hz); HRMS (ESI-TOF) m/z [M + H]<sup>+</sup> 959.3998 calcd for C<sub>52</sub>H<sub>53</sub>B<sub>2</sub>F<sub>4</sub>N<sub>4</sub>O<sub>8</sub> 959.3980. Its byproduct BODIPY 4 was obtained in 6% yield as a red solid. mp (°C) > 235 decomp; <sup>1</sup>H NMR (400 MHz, CD<sub>2</sub>Cl<sub>2</sub>)  $\delta$  9.40 (s, 1H), 7.78 (d, J = 8.3 Hz, 2H), 7.76–7.67 (m, 4H), 7.35 (d, J = 8.3 Hz, 2H), 4.42

#### Scheme 2. Synthesis of BODIPY Dimers 1a, 1b, 2 and 3

(q, J = 7.1 Hz, 4H), 4.35 (q, J = 7.1 Hz, 4H), 2.29 (s, 3H), 2.03 (s, 3H), 2.00 (s, 6H), 1.44–1.37 (m, 15H); <sup>11</sup>B NMR (128 MHz, CD<sub>2</sub>Cl<sub>2</sub>)  $\delta$  0.12 (t, J = 27.6 Hz); HRMS (ESI-TOF) m/z [M + Na]<sup>+</sup> 784.2996 calcd for C<sub>43</sub>H<sub>42</sub>BF<sub>2</sub>N<sub>3</sub>NaO<sub>7</sub> 784.2976.

1,2,6,7-Tetramethyl-3,5-di(ethoxycarbonyl)-8-phenyl-BODIPY **5**. The general procedure was followed with modified molar ratio of reagents: benzaldehyde (47 mg, 0.20 mmol), 2-ethoxycarbonyl-3,4-dimethylpyrrole (66 mg, 0.40 mmol), and DDQ (45 mg, 0.20 mmol). The compound was obtained in 49 mg (53%) yield as a red solid. mp (°C) > 245 decomp; <sup>1</sup>H NMR (CDCl<sub>3</sub>, 400 MHz) δ 7.56–7.52 (m, 3H), 7.28–7.22 (m, 5H), 4.46 (q, J = 7.1 Hz, 4H), 1.99 (s, 6H), 1.43 (t, J = 7.1 Hz, 6H), 1.31 (s, 6H); <sup>13</sup>C NMR (CDCl<sub>3</sub>, 125 MHz) δ 162.24, 148.27, 145.17, 142.09, 134.71, 133.17, 129.71, 129.56, 129.42, 127.49, 61.94, 14.01, 12.19, 9.52; <sup>11</sup>B NMR (CDCl<sub>3</sub>, 128 MHz) δ 0.23 (t, J = 27.7 Hz); HRMS (ESI-TOF) m/z [M + Na] + 491.1933 calcd for  $C_{25}H_{27}BF_2N_2NaO_4$  491.1924.

**2.2. Crystal Data.** Structures of compounds **1b**, **2**, **3**, and **4** were determined from low-temperature diffraction data measured on a Bruker Kappa Apex-II DUO diffractometer with Mo K $\alpha$  ( $\lambda$  = 0.710 73 Å) or Cu K $\alpha$  ( $\lambda$  = 1.541 84 Å) radiation. Intensities were corrected for absorption using

Bruker SADABS. Structures were solved by direct methods and refined using SHELXL2014, with hydrogen atoms placed in calculated positions. Crystal data: 1b,  $C_{56}H_{62}B_2F_4N_4O_{8}$ , M =1016.72, monoclinic, space group I2/a, a = 17.4387(4), b =13.6958(2), c = 21.7973(3) Å,  $\beta = 96.513(2)^{\circ}$ , U =5172.40(16) Å<sup>3</sup>, T = 150 K, Z = 4, Dc = 1.306 g cm<sup>-3</sup>,  $\mu(\text{Mo K}\alpha) = 0.10 \text{ mm}^{-1}$ , 55 742 reflections measured,  $\theta_{\text{max}} =$ 31.5°, 8557 unique ( $R_{int} = 0.045$ ), final R = 0.053 (5997 I > $2\sigma(I)$  data), 370 parameters,  $wR(F^2) = 0.159$  (all data), CCDC 1841069; **2**,  $C_{52}H_{54}B_2F_4N_4O_8$ , M = 960.61, monoclinic, space group  $P2_1/c$ , a = 21.6230(7), b = 11.4575(3), c = 19.1802(6)Å,  $\beta = 91.350(2)^{\circ}$ , U = 4750.5(2) Å<sup>3</sup>, T = 110 K, Z = 4, Dc = 1.343 g cm<sup>-3</sup>,  $\mu$ (Mo K $\alpha$ ) = 0.10 mm<sup>-1</sup>, 28 382 reflections measured,  $\theta_{\text{max}} = 26.5^{\circ}$ , 9764 unique ( $R_{\text{int}} = 0.043$ ), final R = $0.050 (6482 I > 2\sigma(I) \text{ data}), 643 \text{ parameters}, wR(F^2) = 0.130$ (all data), CCDC 1841070; 3,  $C_{52}H_{52}B_2F_4N_4O_8$ , M = 958.59, monoclinic, space group  $P2_1/n$ , a = 14.1888(4), b =20.3677(6), c = 16.9823(5) Å,  $\beta = 94.375(2)^{\circ}$ , U =4893.5(2)Å<sup>3</sup>, T = 100 K, Z = 4, Dc = 1.301 g cm<sup>-3</sup>,  $\mu$ (Cu  $K\alpha$ ) = 0.81 mm<sup>-1</sup>, 47 343 reflections measured,  $\theta_{max}$  = 68.3°, 8865 unique ( $R_{\text{int}} = 0.056$ ), final R = 0.066 (5165  $I > 2\sigma(I)$ data), 643 parameters, $wR(F^2) = 0.196$  (all data), CCDC

FtOOC

COOF

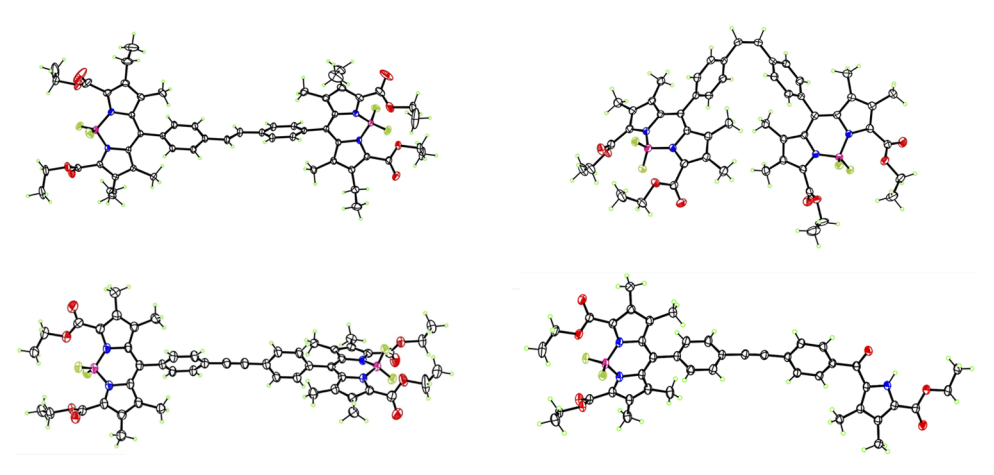


Figure 1. Crystal structures of BODIPYs 1b (top left), 2 (top right), 3 (bottom left), and 4 (bottom right) with 50% ellipsoids.

1841071; 4, C<sub>43</sub>H<sub>42</sub>BF<sub>2</sub>N<sub>3</sub>O<sub>7</sub>, M=761.60, monoclinic, space group  $P2_1/n$ , a=14.2474(3), b=12.0988(3), c=22.9831(5) Å,  $\beta=106.8142(14)^\circ$ , U=3792.37(15)Å<sup>3</sup>, T=100 K, Z=4, Dc = 1.334 g cm<sup>-3</sup>,  $\mu$ (Cu K $\alpha$ ) = 0.80 mm<sup>-1</sup>, 24 738 reflections measured,  $\theta_{\rm max}=69.4^\circ$ , 6884 unique ( $R_{\rm int}=0.033$ ), final R=0.040 (5648  $I>2\sigma(I)$  data), 517 parameters, $\nu R(F^2)=0.111$  (all data), CCDC 1841072.

2.3. Spectroscopy. All UV-visible and fluorescence spectra of BODIPYs were obtained on a UV spectrophotometer and a luminescence spectrophotometer at 298 K, respectively. Ten millimeter path length quartz cuvettes and spectroscopic-grade solvents were used for both of the measurements. Molar absorption coefficients ( $\varepsilon$ ) were calculated from the slope of absorbance versus concentration with absorbance in the range of 0.2-1.0. Fluorescence quantum yields  $(\Phi_f)$  were determined on a series of dilute solutions with absorbance values between 0.02 and 0.06 at a particular excitation wavelength. Rhodamine B (0.70 in methanol) was chosen as external standard for all BODIPYs. The relative fluorescence quantum yields  $(\Phi_f)$  were determined using the equation:  $\Phi_X = \Phi_S(I_X/I_S)(A_S/A_X)(n_X/I_S)$  $(n_s)^2$ , where  $\Phi$  refers to the fluorescence quantum yields, n represents the refractive indexes of the solvents used for the measurement, I refers to the integrated fluorescence intensity, A refers to the corresponding absorbance at the excitation wavelength, and subscripts X and S represent the tested samples and the external standards, respectively.

**2.4. Computational Methods.** The geometries of all compounds and complexes were optimized without symmetry constraints using two methods: CAM-B3LYP/6-31+G(d,p)<sup>70</sup> and M06-2X/6-31+G(d,p).<sup>71</sup> The stationary points on the potential energy surface were confirmed with frequency calculations. The absorption spectra were calculated in tetrahydrofuran (THF) using the time-dependent density functional theory (TD-DFT) method<sup>72</sup> and both CAM-B3LYP/6-31+G(d) and M06-2X/6-31+G(d) levels, as recommended in several papers and reviews.<sup>73-75</sup> The solvent effects were taken into account using the Polarized Continuum Model (PCM).<sup>76,77</sup> All calculations were performed using the Gaussian 09 program package.<sup>78</sup>

# 3. RESULTS AND DISCUSSION

**3.1. Synthesis of BODIPY Dimers.** The synthetic route to the (E)-ethenyl (1a,b), (Z)-ethenyl- (2), and ethynyl- (3) BODIPY dimers, from the corresponding bis-benzaldehydes

cores, is shown in Scheme 2. On the one hand, the (E)-4,4'bromostilbene was synthesized as the main product from the McMurray reaction of 4-bromobenzaldehyde, as previously reported. <sup>64</sup> On the other hand, the (Z)-4,4'-bromostilbene was obtained as the major product from the one-pot Kornblumtype oxidation and in situ Wittig reaction of 4-bromobenzyl bromide. 61 Both these reactions required the separation of the main regioisomer, which was readily accomplished by column chromatography. Formylation of the pure (E)- or (Z)-4,4'bromostilbene isomers using n-BuLi and dimethylformamide (DMF) at -78 °C gave the corresponding (E)- and (Z)-4,4'formylstilbenes, in 57 and 52% yields, respectively.<sup>63</sup> Condensation of the (E)-4,4'-formylstilbene with 2-ethoxvcarbonyl-3,4-dimethylpyrrole or 2-ethoxycarbonyl-3-ethyl-4methylpyrrole, 62,66 followed by DDQ oxidation and boron complexation with boron trifluoride etherate under basic conditions, gave the (E)-ethenyl-linked BODIPYs 1a and 1b, respectively, in 31-34% overall yields. With a similar procedure, the (Z)-ethenyl BODIPY dimer 2 was obtained from (Z)-4,4'-formylstilbene in 23% yield. The ethoxycarbonyl-functionalized pyrroles were chosen to minimize side reactions and to increase the stability of the targeted dimers. Furthermore, the ethoxycarbonyl functionalities could be used subsequently for conjugation upon ester cleavage.

Previously reported ethynyl-linked BODIPY dimers were prepared from BODIPY monomers via alkyne metathesis or Sonogashira cross-coupling reactions. S9,60 Our new alternative synthetic route involved the synthesis of the linker first followed by assembly of the BODIPY units, as in the case of the (E,Z)-ethenyl dimers (Scheme 2). The 4,4'-(ethyne-1,2-diyl)dibenzaldehyde core was synthesized in one step through Pd(0)-catalyzed diarylation of propiolic acid, as previously reported. Condensation of the dibenzaldehyde with 2-ethoxycarbonyl-3,4-dimethylpyrrole, followed by oxidation and boron complexation, gave ethynyl-linked BODIPY 3 in 28% yield.

One of the side products observed in all the above synthesis of dimers was a mono-BODIPY ketopyrrole, obtained from oxidation at the benzylic position. In the case of the ethynyllinked dimer 3, the side product 4 was isolated, and its structure was characterized by <sup>1</sup>H NMR, HRMS, and by X-ray crystallography. Such ketopyrrole byproducts have been previously observed during the synthesis of meso-phenylbridged BODIPY dimers. <sup>67</sup>

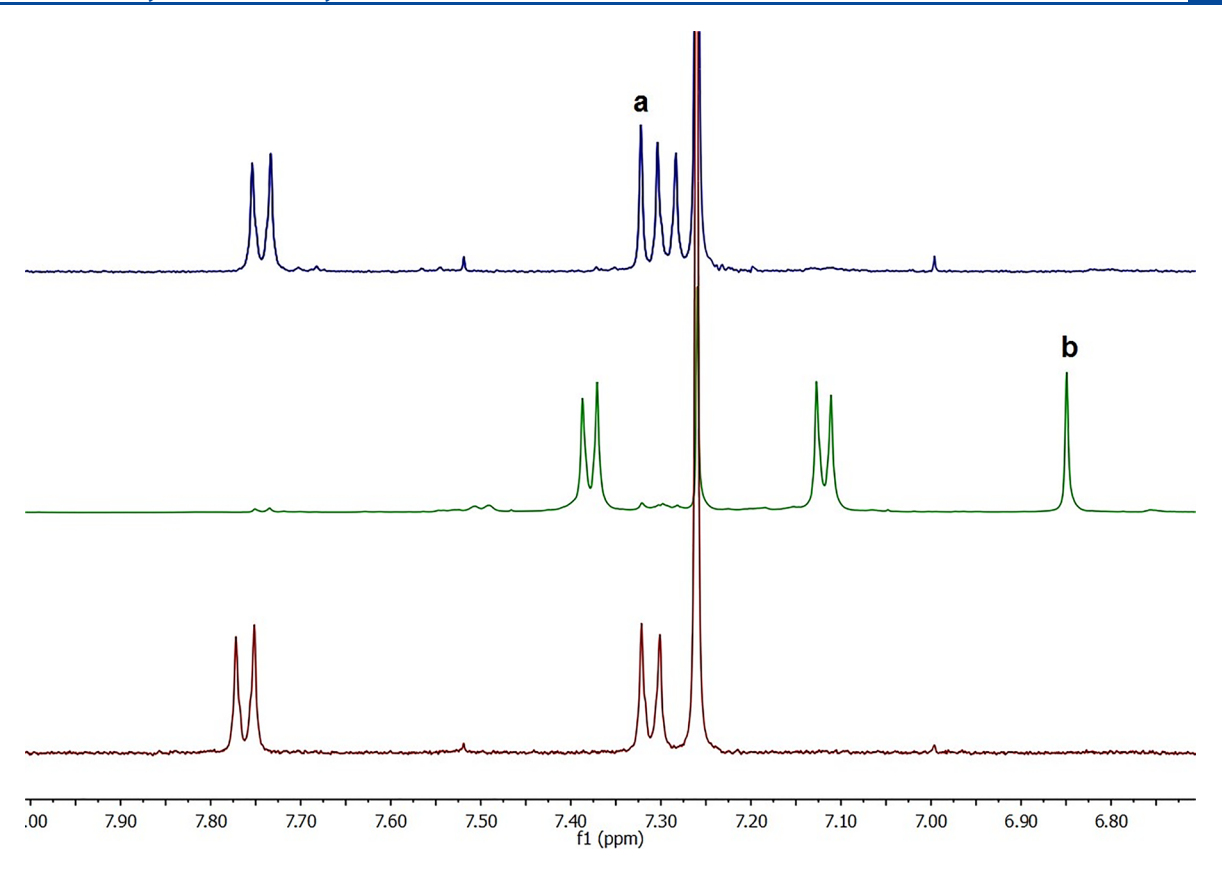


Figure 2. <sup>1</sup>H NMR spectrum (400 MHz) of dimers 1a (top), 2 (middle), and 3 (bottom) in CDCl<sub>3</sub> at 315 K. The (a) and (b) signals correspond to the olefinic protons of 1a and 2, respectively.

3.2. X-ray Structure Characterization. Crystals of BODIPYs 1b, 2, 3, and 4 suitable for X-ray analysis were obtained from slow evaporation of CH2Cl2, and their structures are shown in Figure 1. Over the four structures, B-F distances fell within the range of 1.3663(17)-1.385(5) Å with mean value 1.378 Å, while values for B-N distances were 1.552(5)-1.566(2) and 1.558 Å. Central C=C distances were 1.332(3) Å in 1b and 1.323(3) Å in 2, while triple-bond distances were shorter, 1.196(5) Å in 3 and 1.198(2) Å in 4. The E isomer 1b lies on a crystallographic twofold axis and thus has one independent BODIPY group. On the one hand, its C<sub>3</sub>N<sub>2</sub>B core has a twisted conformation, in which the B lies +0.192 Å and one N lies -0.165 Å out of the plane of the other four atoms. On the other hand, the Z isomer 2 has two independent BODIPYs, and both have C<sub>3</sub>N<sub>2</sub>B cores with envelope conformations, the B atoms lying 0.314 and 0.317 Å out of the best planes of the other five atoms. The ethynyllinked dimer 3 also has its C<sub>3</sub>N<sub>2</sub>B cores in similar envelope conformations, the B atoms lying 0.217 and 0.288 Å out of the best planes of the other five atoms. The single BODIPY in ethynyl-linked 4 has a similar envelope core with the B atom 0.327 Å out of plane. These envelopes impart an overall bowed conformation on the C<sub>0</sub>N<sub>2</sub>B moieties, with the two pyrroles tilted in the same direction out of the central plane. They also cause the two F atoms on each BF2 unit to lie out of plane by different amounts, 0.57 and 1.61 Å (averages of five values over structures 2, 3, and 4). The corresponding tilt of the BF<sub>2</sub> group in 1b is more pronounced, with out-of-plane deviations 0.46 and 1.65 Å for its two F atoms.

The phenyl groups of the linkers at the meso(8)-positions form similar dihedral angles with the BODIPY core planes over

the four reported structures. In **1b**, this dihedral angle is  $65.6^{\circ}$ , in **2** the two values are 75.3 and 83.0°, in **3** they are 71.6 and 78.7°, and in **4**, the dihedral angle is  $76.9^{\circ}$ . The two phenyl groups of the linkers in dimers **1b**, **2**, and **3** exhibit a wide range of deviations from coplanarity, the smallest observed for the diphenylethynyl and the largest for the (Z)-diphenylethene linker: in the (E)-stilbene linker of **1b**, the two phenyl planes form a dihedral angle of 23.8°, in the (Z)-stilbene of **2**, the value is 59.2°, and in the diphenylethyne linkers of **3** the values decreases to 20.0°. In the case of **4**, the angle is 85.0°due to the extended conjugation with the ketopyrrole.

The packing of molecules of **1b** feature intermolecular C—H···O interactions and C—H···F interactions, which involve the central olefinic hydrogen atoms. We did not observe stacking of either phenyl groups or BODIPY cores in any of the BODIPY dimers, as no centroid···centroid distances were shorter than 6 Å. Although in 3 no stacking of phenyl groups nor BODIPYs were observed, one pyrrole unit has a perpendicular spacing of 3.63 Å with an inversion related one. However, the centroids of these rings are slipped by 1.93 Å, such that the distance between centroids is 4.11 Å. The predominant contacts involve ester groups and a few edge-on C—H···F contacts involving phenyl groups. Similarly, in 4 there is no stacking of phenyl nor BODIPY planes, but intermolecular contacts generally involve esters and edge-on phenyl C—H···F interactions.

**3.3. Spectroscopic Characterization.** The BODIPY dimers **1a**, **1b**, **2**, **3**, and 1,2,6,7-tetramethyl-3,5-di-(ethoxycarbonyl)-8-phenyl-BODIPY **5** were characterized by  $^{1}$ H,  $^{11}$ B, and  $^{13}$ C NMR. All BODIPY derivatives exhibited a triplet in their  $^{11}$ B-NMR at  $\sim$ 0.20 ppm with ca.  $I_{BF} = 28$  Hz.

Table 1. Experimental and TD-DFT Calculated Spectroscopic Properties of BODIPYs in  $\mathrm{THF}^a$ 

		leading transition(s)	E (eV)		$\lambda_{\mathrm{abs}} \; (\mathrm{nm})$			oscillator strength		$\log \varepsilon$	$\begin{pmatrix} \lambda_{\mathrm{em}} \\ (\mathrm{nm}) \end{pmatrix}$	$\Phi_{ m f}^{b}$	Stokes shift (cm <sup>-1</sup> )
method			(a)	(b)	(a)	(b)	exp	(a)	(b)	exp	exp	exp	exp
monomer	$S_1$	HOMO→LUMO	2.759	2.718	449.39	456.23	534	0.6002	0.5811	4.19	562	0.88	933
	$S_2$	HOMO−1→ LUMO	3.4339	3.4146	361.06	363.10		0.1447	0.1534				
dimer 1a	$S_1$	HOMO−1→ LUMO	2.755	2.709	449.97	457.72	534	0.0876	0.1503	4.15	561	0.56	901
		HOMO→ LUMO+1											
	$S_1'$	HOMO→ LUMO+1	2.765	2.717	448.49	456.33		1.0843	0.9765				
		HOMO−1→ LUMO											
	$S_2$	HOMO−2→ LUMO	3.3902	3.2266	365.71	384.26		0.1343	0.4824				
dimer 2	$S_1$	HOMO−1→ LUMO	2.757		449.6		534	0.3153		4.38	560	0.44	869
		HOMO→ LUMO+1											
	$S_1'$	HOMO→ LUMO+1	2.764		448.59			0.8398					
		HOMO−1→ LUMO											
	$S_2$	HOMO−2→ LUMO	3.4359		360.85			0.1219					
dimer 3	$S_1$	HOMO−1→ LUMO	2.749	2.649	451.1	468.01	534	0.0411	0.3637	4.41	559	0.32	838
		HOMO→ LUMO+1											
	$S_1{}'$	HOMO→ LUMO+1	2.758	2.659	449.55	466.31		1.1334	0.7099				
		HOMO−1→ LUMO											
	$S_2$	HOMO−2→ LUMO	3.427	2.7874	361.78	441.81		0.0571	0.3218				
_													

 $<sup>^</sup>a$ Two computational methods were used: (a) CAM-B3LYP/6-31+G(d) and (b) M06-2X/6-31+G(d). All calculations were done in THF.  $^b$ Rhodamine B (0.70 in ethanol) was used as standard. The error associated with the fluorescence quantum yield determination is 0.02.

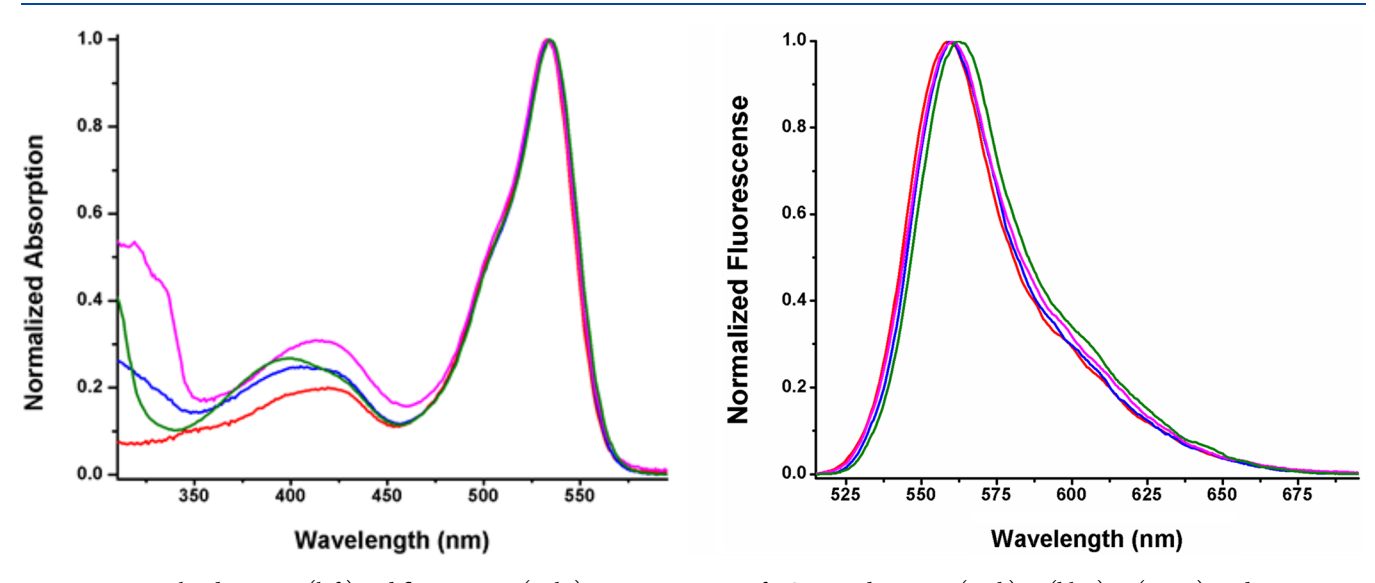


Figure 3. Normalized UV-vis (left) and fluorescence (right) emission spectra of BODIPY dimers 1a (pink), 2 (blue), 3 (green), and monomer 5 (red) in THF at room temperature.

The  $^1$ H NMR spectra displayed the olefinic protons for the E-dimers **1a** and **1b** downfield shifted at  $\sim$ 7.32 ppm relative to the Z-dimer **2** olefinic protons, which appear at 6.85 ppm, as shown in Figure 2. The singlet peak of the olefinic protons shows the symmetry of the BODIPY dimers. The phenyl

protons in E-dimers 1a and 1b appear downfield shifted compared with those of the Z-dimer 2 due to the shielding effect of the phenyl group as a result of the cis geometry (see Figure 1). Similarly, the phenyl protons of ethynyl-linked 3 show similar chemical shifts to those of E-dimers 1a and 1b.

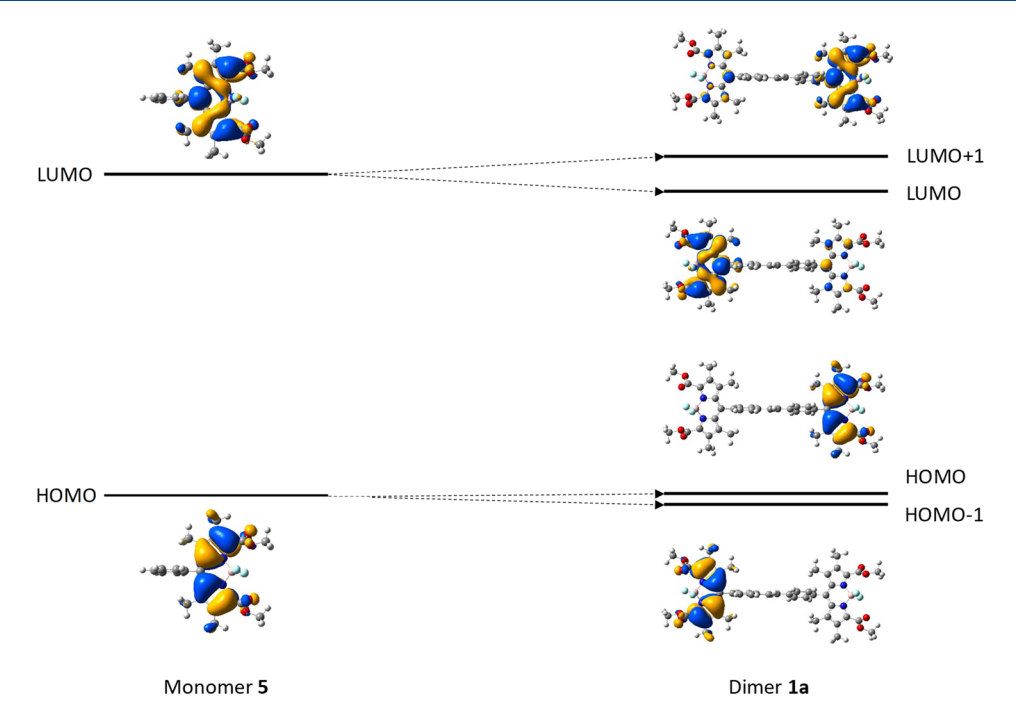


Figure 4. Splitting of monomer's HOMO and LUMO into two orbitals each in dimer 1a (0.001 eV for HOMO and 0.010 eV for LUMO). Similar splitting is observed in dimers 2 (0.011 eV for HOMO and 0.021 eV for LUMO) and 3 (0.001 eV for HOMO and 0.007 eV for LUMO).

The ethynyl-linked BODIPY dimer 3 shows a single peak at 90.24 ppm in <sup>13</sup>C NMR, indicating the ethynyl group is incorporated in the symmetric structure.

The absorption and emission spectra of BODIPYs 1a, 2, 3, and 5 in THF were investigated, and the results are summarized in Table 1 and Figure 3. Strong  $S_0 \rightarrow S_1$  transitions with high molar absorption coefficients were observed for all compounds. The weaker and broader absorption band at lower wavelength (400 nm) is attributed to  $S_0 \rightarrow S_n$  ( $n \ge 2$ ) transitions of the BODIPY moiety. This was confirmed with TD-DFT calculations as discussed in Section 3.4. Absorption and emission maxima are almost identical for all three BODIPY dimers and the monomer at  $\lambda = 534$  nm and  $\lambda =$ 560 nm, respectively (Table 1). The orthogonal structure of the meso-phenyl and the BODIPY cores hampered the electronic conjugation through bonds between the stilbene and BODIPY moieties. Intramolecular stacking was not observed between the two independent BODIPY units in the (Z)-ethenyl-linked BODIPY dimer, as indicated by the lack of the shifted absorption bands as described in the Kasha model, which characterize a stacked monomer pair.<sup>68</sup> In the case of dimers 1aand 1b, J-type or H-type aggregation is not observed, because the BODIPY units are not closely positioned and because of the existence of two free rotation bonds within the linker. The BODIPY monomer 5 exhibits relatively higher fluorescence quantum yield ( $\Phi = 0.88$ ) compared with all dimers. The symmetry-breaking intramolecular charge transfer (ICT) probably occurs upon the formation of nonemissive charge-transfer state in dimers bearing identical BODIPY units, resulting in the lower fluorescence quantum yields of the dimers relative to the monomer.  $^{69}$  Among the dimers, the (E)ethenyl linked dimer 1a displayed the highest fluorescence quantum yield ( $\Phi = 0.56$ ).

**3.4. Computational Study.** The geometries, energies, molecular orbitals (MOs), and UV—vis absorption properties of BODIPY dimers **1a**, **2**, **3** (Scheme 2) and monomer **5** were

modeled computationally using the corresponding methyl esters. The coordinates of the optimized structures are given in Tables S1–S3 of the Supporting Information. In agreement with the X-ray structure results reported above, the phenyl groups of the linkers in dimers 1a, 2, and 3 exhibit a wide range of deviations from coplanarity. The difference with the experiment is that dimer 3 is nearly planar (dihedral angle between the phenyl planes of only  $1-2^{\circ}$ ). This difference might be due to the modeling in solution (THF). In agreement with the experiment, the BF<sub>2</sub> group is tilted outside the BODIPY core plane for all modeled compounds. In addition, the phenyl groups of the linkers are nearly perpendicular to the BODIPY core planes (calculated dihedral angle of  $81-85^{\circ}$  in dimer 1a,  $80-91^{\circ}$  in dimer 2, and  $85-89^{\circ}$  in dimer 3).

The shapes and the energies of the molecular orbitals involved in leading transitions for the monomer and all three dimers are shown in Figures S24-S27 of the Supporting Information. It can be seen that, upon formation of the dimer, the highest occupied molecular orbital (HOMO) of the monomer splits into two orbitals: HOMO and HOMO-1 (one per each monomer unit). Similarly, the lowest unoccupied molecular orbital (LUMO) of the monomer splits into LUMO and LUMO+1 in the dimer (Figure 4). The two new orbitals are similar in energy but are not degenerate. For all dimers, the energy splitting is more pronounced in the LUMO than in the HOMO. The energy splitting is the greatest in the case of dimer 2 (0.011 eV for HOMO and 0.021 eV for LUMO), which could be expected based on the greatest deviation from planarity of the linker and the two meso-phenyl groups in this case. For dimers 1a and 3, the HOMO splitting is negligible (0.001 eV in both cases). The LUMO splitting is greater (0.010 and 0.007 eV, respectively) but still smaller than the one observed for dimer 2. The observed trends are valid regardless of the functional used for the calculation (CAM-B3LYP or M06-2X).

Table 1 gives the TD-DFT calculated excitation energies, wavelengths, and oscillator strengths for monomer 5 and dimers 1a, 2, and 3. Because of the above-discussed splitting of the MOs, instead of a single  $S_0 \rightarrow S_1$  transition, as in the monomer, two transitions exist for all dimers:  $S_0 \rightarrow S_1$  and  $S_0 \rightarrow$ S'1, each associated with a separate monomer unit in the dimer. The absorption wavelengths of the two peaks are so close to each other that experimentally, only one peak is observed. The leading transition in the monomer is HOMO→ LUMO. Upon dimerization, this transition is split into two transitions both including HOMO−1→LUMO and HOMO→ LUMO+1, but in one of them  $(S_0 \rightarrow S_1)$  the first is predominant, whereas in the other one  $(S_0 \rightarrow S'_1)$ , the second is predominant. This behavior is observed in all of the studied dimers. Interestingly, the  $S_0 \rightarrow S'_1$  transition (where HOMO $\rightarrow$ LUMO+1 is predominant) has significantly higher oscillator strength than the  $S_0 \rightarrow S_1$  transition. This is especially true for the more symmetric dimers 1a and 3. Comparison with the shapes of the orbitals demonstrates that HOMO-1→LUMO and HOMO→LUMO+1 transitions correspond to the HOMO-LUMO transitions in the separate monomer unit (see Supporting Information, Figures S24-S27).

The above results show that the leading transitions have little mixing, which might explain the experimentally observed smaller quantum yields for the dimers compared to the monomer. The excitation energies of the dimers are very similar to the excitation energies of the monomer with a shift of only ~1 nm. This is in agreement with the experimentally observed values, with little to no change in the maximum absorption wavelengths upon dimerization. Moreover, since the MOs associated with the linker part of the dimers are not involved in the maximum intensity transition (these are HOMO-2 in all dimers, see Figures S24-S27 of the Supporting Information), it is not surprising that all dimers demonstrate very similar maximum absorption and maximum emission wavelengths. The HOMO-2 orbitals play a major part in the shorter wavelengths  $S_0 \rightarrow S_2$  transition. This is in agreement with the experimentally observed difference in the absorption spectra at shorter wavelengths (see Figure 3).

Interestingly, it appears that the CAM-B3LYP functional better predicts the absorption wavelengths of these compounds. On the one hand, M06-2X gives large shifts for all dimers, especially for dimer 3. On the other hand, M06-2X appears to give more meaningful oscillator strengths. DFT calculations at the CAM-B3LYP level also showed that dimer 1a is slightly lower in energy than dimers 2 by 4.7 kcal/mol.

#### 4. CONCLUSIONS

A synthetic route was developed for the preparation of four meso-meso BODIPY dimers with different linkers ((E)ethenyl, (Z)-ethenyl, and ethynyl diphenyl). The synthesis of the precursor dialdehyde cores prior to the formation of the BODIPY units allowed the easy incorporation of (E)- or (Z)ethenyl stereochemistry into the linker and facilitated their purification. The structures of the linkers and the arrangement of the BODIPY units in the dimers were investigated by NMR spectroscopy, X-ray crystallography, and DFT calculations. The ethynyl-linked dimer displayed the most planar conformation, closely followed by the (E)-ethynyl dimers, with the linker phenyl groups nearly perpendicular to the BODIPY core planes for all dimers. Intramolecular aggregation of BODIPY units was not observed, and all BODIPYs displayed similar absorption and emission wavelengths. Among the dimers, the

(E)-ethenyl linked one showed the highest fluorescence quantum yield.

## ASSOCIATED CONTENT

# Supporting Information

The Supporting Information is available free of charge on the ACS Publications website at DOI: 10.1021/acs.jpca.8b05149.

<sup>1</sup>H, <sup>13</sup>C, and <sup>11</sup>B NMR spectra, ESI mass spectra (PDF) Cartesian coordinates of the optimized structures of BODIPYs 1a, 2, 3, and 5. Frontier molecular orbitals of BODIPYs 1a, 2, 3, and 5. X-ray data for BODIPYs 1b, 2, 3, and 4 (CIF)

#### AUTHOR INFORMATION

## **Corresponding Author**

\*E-mail: vicente@lsu.edu.

ORCID ®

Ning Zhao: 0000-0003-3699-3369

Petia Bobadova-Parvanova: 0000-0002-1965-419X

Frank R. Fronczek: 0000-0001-5544-2779 M. Graça H. Vicente: 0000-0002-4429-7868

The authors declare no competing financial interest.

#### ACKNOWLEDGMENTS

This work was supported by the National Science Foundation Grant No. CHE 1800126. The authors are thankful to the Louisiana State Univ. High Performance Computing Center (http://www.hpc.lsu.edu) for use of its computational resources in conducting this research.

## REFERENCES

- (1) Loudet, A.; Burgess, K. BODIPY Dyes and Their Derivatives: Syntheses and Spectroscopic Properties. Chem. Rev. 2007, 107, 4891-
- (2) Ulrich, G.; Ziessel, R.; Harriman, A. The Chemistry of Fluorescent BODIPY Dyes: Versatility Unsurpassed. Angew. Chem., Int. Ed. 2008, 47, 1184-1201.
- (3) Boens, N.; Leen, V.; Dehaen, W. Fluorescent Indicators Based on BODIPY. Chem. Soc. Rev. 2012, 41, 1130-1172.
- (4) Lu, H.; Mack, J.; Yang, Y.; Shen, Z. Structural Modification Strategies for the Rational Design of Red/NIR Region BODIPYs. Chem. Soc. Rev. 2014, 43, 4778-4823.
- (5) Ni, Y.; Wu, J. Far-Red and Near Infrared BODIPY Dyes: Synthesis and Applications for Fluorescent pH Probes and Bio-Imaging. Org. Biomol. Chem. 2014, 12, 3774-3791.
- (6) Boens, N.; Verbelen, B.; Dehaen, W. Postfunctionalization of the BODIPY Core: Synthesis and Spectroscopy. Eur. J. Org. Chem. 2015, 2015, 6577-6595.
- (7) Kowada, T.; Maeda, H.; Kikuchi, K. BODIPY-Based Probes for The Fluorescence Imaging of Biomolecules in Living Cells. Chem. Soc. Rev. 2015, 44, 4953-4972.
- (8) Gómez-Durán, C. F.; Esnal, I.; Valois-Escamilla, I.; Urías-Benavides, A.; Bañuelos, J.; Lopez Arbeloa, I.; García-Moreno, I.; Peña-Cabrera, E. Near-IR BODIPY Dyes à la Carte-Programmed Orthogonal Functionalization of Rationally Designed Building Blocks. Chem. - Eur. J. 2016, 22, 1048-1061.
- (9) Nierth, A.; Kobitski, A. Y.; Nienhaus, G. U.; Jäschke, A. Anthracene-BODIPY Dyads as Fluorescent Sensors for Biocatalytic Diels-Alder Reactions. J. Am. Chem. Soc. 2010, 132, 2646-2654.
- (10) Yin, S.; Leen, V.; Van Snick, S.; Boens, N.; Dehaen, W. A Highly Sensitive, Selective, Colorimetric and Near-Infrared Fluorescent Turn-On Chemosensor for Cu<sup>2+</sup> Based on BODIPY. Chem. Commun. 2010, 46, 6329-6331.

- (11) Kim, H. N.; Ren, W. X.; Kim, J. S.; Yoon, J. Fluorescent and Colorimetric Sensors for Detection of Lead, Cadmium, and Mercury Ions. *Chem. Soc. Rev.* **2012**, *41*, 3210–3244.
- (12) Kong, X.; Su, F.; Zhang, L.; Yaron, J.; Lee, F.; Shi, Z.; Tian, Y.; Meldrum, D. R. A Highly Selective Mitochondria-Targeting Fluorescent K<sup>+</sup> Sensor. *Angew. Chem., Int. Ed.* **2015**, *54*, 12053–12057.
- (13) Christianson, A. M.; Gabbaï, F. P. Anion Sensing with a Lewis Acidic BODIPY-Antimony (V) Derivative. *Chem. Commun.* **2017**, *53*, 2471–2474.
- (14) Miao, W.; Dai, E.; Sheng, W.; Yu, C.; Hao, E.; Liu, W.; Wei, Y.; Jiao, L. Direct Synthesis of Dipyrrolyldipyrrins from SNAr Reaction on 1, 9-Dihalodipyrrins with Pyrroles and Their NIR Fluorescence "Turn-On" Response to Zn<sup>2+</sup>. Org. Lett. **2017**, 19, 6244–6247.
- (15) Xia, H.-C.; Xu, X.-H.; Song, Q.-H. BODIPY-Based Fluorescent Sensor for the Recognization of Phosgene in Solutions and in Gas Phase. *Anal. Chem.* **2017**, *89*, 4192–4197.
- (16) Coskun, A.; Deniz, E.; Akkaya, E. U. Effective PET and ICT Switching of Boradiazaindacene Emission: a Unimolecular, Emission-Mode, Molecular Half-Subtractor with Reconfigurable Logic Gates. *Org. Lett.* **2005**, *7*, 5187–5189.
- (17) Cao, J.; Zhao, C.; Wang, X.; Zhang, Y.; Zhu, W. Target-Triggered Deprotonation of 6-Hydroxyindole-Based BODIPY: Specially Switch on NIR Fluorescence Upon Selectively Binding to Zn<sup>2+</sup>. Chem. Commun. **2012**, 48, 9897–9899.
- (18) Kolemen, S.; Işık, M.; Kim, G. M.; Kim, D.; Geng, H.; Buyuktemiz, M.; Karatas, T.; Zhang, X. F.; Dede, Y.; Yoon, J.; et al. Intracellular Modulation of Excited-State Dynamics in a Chromophore Dyad: Differential Enhancement of Photocytotoxicity Targeting Cancer Cells. *Angew. Chem., Int. Ed.* **2015**, *54*, 5340–5344.
- (19) Xu, K.; Zhao, J.; Cui, X.; Ma, J. Photoswitching of Triplet—Triplet Annihilation Upconversion Showing Large Emission Shifts Using a Photochromic Fluorescent Dithienylethene-BODIPY Triad as a Triplet Acceptor/Emitter. Chem. Commun. 2015, 51, 1803—1806.
- (20) Zhao, C.; Zhang, X.; Li, K.; Zhu, S.; Guo, Z.; Zhang, L.; Wang, F.; Fei, Q.; Luo, S.; Shi, P.; et al. Forster Resonance Energy Transfer Switchable Self-Assembled Micellar Nanoprobe: Ratiometric Fluorescent Trapping of Endogenous H<sub>2</sub>S Generation via Fluvastatin-Stimulated Upregulation. J. Am. Chem. Soc. 2015, 137, 8490–8498.
- (21) Bura, T.; Leclerc, N.; Fall, S.; Lévêque, P.; Heiser, T.; Retailleau, P.; Rihn, S.; Mirloup, A.; Ziessel, R. High-Performance Solution-Processed Solar Cells and Ambipolar Behavior in Organic Field-Effect Transistors with Thienyl-BODIPY Scaffoldings. *J. Am. Chem. Soc.* 2012, 134, 17404–17407.
- (22) Chen, J. J.; Conron, S. M.; Erwin, P.; Dimitriou, M.; McAlahney, K.; Thompson, M. E. High-Efficiency BODIPY-Based Organic Photovoltaics. *ACS Appl. Mater. Interfaces* **2015**, *7*, 662–669.
- (23) Wu, W.; Guo, H.; Wu, W.; Ji, S.; Zhao, J. Organic Triplet Sensitizer Library Derived from a Single Chromophore (BODIPY) with Long-Lived Triplet Excited State for Triplet—Triplet Annihilation Based Upconversion. J. Org. Chem. 2011, 76, 7056—7064.
- (24) Erbas-Cakmak, S.; Akkaya, E. U. Toward Singlet Oxygen Delivery at a Measured Rate: a Self-Reporting Photosensitizer. *Org. Lett.* **2014**, *16*, 2946–2949.
- (25) Huang, L.; Yang, W.; Zhao, J. Switching of the Triplet Excited State of Styryl 2, 6-Diiodo-BODIPY and its Application in Acid-Activatable Singlet Oxygen Photosensitizing. *J. Org. Chem.* **2014**, 79, 10240–10255.
- (26) Gibbs, J. H.; Zhou, Z.; Kessel, D.; Fronczek, F. R.; Pakhomova, S.; Vicente, M. G. H. Synthesis, Spectroscopic, and In Vitro Investigations of 2, 6-Diiodo-BODIPYs with PDT and Bioimaging Applications. *J. Photochem. Photobiol.*, B **2015**, 145, 35–47.
- (27) Neelakandan, P. P.; Jiménez, A.; Thoburn, J. D.; Nitschke, J. R. An Autocatalytic System of Photooxidation-Driven Substitution Reactions on a  ${\rm Fe^{II}}_4{\rm L}_6$  Cage Framework. *Angew. Chem., Int. Ed.* **2015**, *54*, 14378–14382.
- (28) Lee, J.-S.; Kang, N.-y.; Kim, Y. K.; Samanta, A.; Feng, S.; Kim, H. K.; Vendrell, M.; Park, J. H.; Chang, Y.-T. Synthesis of a BODIPY

- Library and its Application to the Development of Live Cell Glucagon Imaging Probe. J. Am. Chem. Soc. 2009, 131, 10077–10082.
- (29) Hendricks, J. A.; Keliher, E. J.; Wan, D.; Hilderbrand, S. A.; Weissleder, R.; Mazitschek, R. Synthesis of [18F] BODIPY: Bifunctional Reporter for Hybrid Optical/Positron Emission Tomography Imaging. *Angew. Chem., Int. Ed.* **2012**, *51*, 4603–4606.
- (30) Vázquez-Romero, A.; Kielland, N.; Arévalo, M. J.; Preciado, S.; Mellanby, R. J.; Feng, Y.; Lavilla, R.; Vendrell, M. Multicomponent Reactions for De Novo Synthesis of BODIPY Probes: In Vivo Imaging of Phagocytic Macrophages. J. Am. Chem. Soc. 2013, 135, 16018–16021.
- (31) Üçüncü, M.; Emrullahoğlu, M. A BODIPY-Based Reactive Probe for the Detection of Au (III) Species and its Application to Cell Imaging. *Chem. Commun.* **2014**, *50*, 5884–5886.
- (32) Yu, C.; Wu, Q.; Wang, J.; Wei, Y.; Hao, E.; Jiao, L. Red to Near-Infrared Isoindole BODIPY Fluorophores: Synthesis, Crystal Structures, and Spectroscopic and Electrochemical Properties. *J. Org. Chem.* **2016**, *81*, 3761–3770.
- (33) Xuan, S.; Zhao, N.; Ke, X.; Zhou, Z.; Fronczek, F. R.; Kadish, K. M.; Smith, K. M.; Vicente, M. G. H. Synthesis and Spectroscopic Investigation of a Series of Push—Pull Boron Dipyrromethenes (BODIPYs). J. Org. Chem. 2017, 82, 2545—2557.
- (34) Zhao, N.; Williams, T. M.; Zhou, Z.; Fronczek, F. R.; Sibrian-Vazquez, M.; Jois, S. D.; Vicente, M. G. H. Synthesis of BODIPY-Peptide Conjugates for Fluorescence Labeling of EGFR Over-expressing Cells. *Bioconjugate Chem.* **2017**, 28, 1566–1579.
- (35) Zhao, N.; Xuan, S.; Zhou, Z.; Fronczek, F. R.; Smith, K. M.; Vicente, M. G. H. Synthesis and Spectroscopic and Cellular Properties of Near-IR [a] Phenanthrene-Fused 4, 4-Difluoro-4-Bora-3a, 4a-Diaza-S-Indacenes. *J. Org. Chem.* **2017**, *82*, 9744–9750.
- (36) Bröring, M.; Krüger, R.; Link, S.; Kleeberg, C.; Köhler, S.; Xie, X.; Ventura, B.; Flamigni, L. Bis(BF<sub>2</sub>)-2, 2'-Bidipyrrins-(BisBODIPYs): Highly Fluorescent BODIPY Dimers with Large Stokes Shifts. *Chem. Eur. J.* **2008**, *14*, 2976–2983.
- (37) Nepomnyashchii, A. B.; Bröring, M.; Ahrens, J.; Bard, A. J. Chemical and Electrochemical Dimerization of BODIPY Compounds: Electrogenerated Chemiluminescent Detection of Dimer Formation. J. Am. Chem. Soc. 2011, 133, 19498–19504.
- (38) Nepomnyashchii, A. B.; Bröring, M.; Ahrens, J.; Bard, A. J. Synthesis, Photophysical, Electrochemical, and Electrogenerated Chemiluminescence Studies. Multiple Sequential Electron Transfers in BODIPY Monomers, Dimers, Trimers, and Polymer. *J. Am. Chem. Soc.* 2011, 133, 8633–8645.
- (39) Rihn, S.; Erdem, M.; De Nicola, A.; Retailleau, P.; Ziessel, R. Phenyliodine (III) Bis(Trifluoroacetate)(PIFA)-Promoted Synthesis of BODIPY Dimers Displaying Unusual Redox Properties. *Org. Lett.* **2011**, *13*, 1916–1919.
- (40) Ahrens, J.; Böker, B.; Brandhorst, K.; Funk, M.; Bröring, M. Sulfur-Bridged BODIPY Dyemers. *Chem. Eur. J.* **2013**, *19*, 11382–11395.
- (41) Kesavan, P. E.; Das, S.; Lone, M. Y.; Jha, P. C.; Mori, S.; Gupta, I. Bridged Bis-BODIPYs: Their Synthesis, Structures and Properties. *Dalton Trans.* **2015**, *44*, 17209–17221.
- (42) Hayashi, Y.; Yamaguchi, S.; Cha, W. Y.; Kim, D.; Shinokubo, H. Synthesis of Directly Connected BODIPY Oligomers through Suzuki—Miyaura Coupling. *Org. Lett.* **2011**, *13*, 2992–2995.
- (43) Wakamiya, A.; Murakami, T.; Yamaguchi, S. Benzene-Fused BODIPY and Fully-Fused BODIPY Dimer: Impacts of the Ring-Fusing at the B Bond in the BODIPY Skeleton. *Chem. Sci.* **2013**, *4*, 1002–1007.
- (44) Yokoi, H.; Wachi, N.; Hiroto, S.; Shinokubo, H. Oxidation of 2-Amino-Substituted BODIPYs Providing Pyrazine-Fused BODIPY Trimers. *Chem. Commun.* **2014**, *50*, 2715–2717.
- (45) Wang, J.; Wu, Q.; Wang, S.; Yu, C.; Li, J.; Hao, E.; Wei, Y.; Mu, X.; Jiao, L. Conformation-Restricted Partially and Fully Fused BODIPY Dimers as Highly Stable Near-Infrared Fluorescent Dyes. *Org. Lett.* **2015**, *17*, 5360–5363.
- (46) Yu, C.; Jiao, L.; Li, T.; Wu, Q.; Miao, W.; Wang, J.; Wei, Y.; Mu, X.; Hao, E. Fusion and Planarization of BisBODIPY: A New

- Family of Photostable Near Infrared Dyes. *Chem. Commun.* **2015**, *51*, 16852–16855.
- (47) Coskun, A.; Akkaya, E. U. Ion Sensing Coupled to Resonance Energy Transfer: a Highly Selective and Sensitive Ratiometric Fluorescent Chemosensor for Ag (I) by a Modular Approach. J. Am. Chem. Soc. 2005, 127, 10464–10465.
- (48) Barin, G.; Yilmaz, M. D.; Akkaya, E. U. Boradiazaindacene (BODIPY)-Based Building Blocks for The Construction of Energy Transfer Cassettes. *Tetrahedron Lett.* **2009**, *50*, 1738–1740.
- (49) Bozdemir, O. A.; Cakmak, Y.; Sozmen, F.; Ozdemir, T.; Siemiarczuk, A.; Akkaya, E. U. Synthesis of Symmetrical Multichromophoric BODIPY Dyes and Their Facile Transformation into Energy Transfer Cassettes. *Chem. Eur. J.* **2010**, *16*, 6346–6351.
- (50) Cakmak, Y.; Kolemen, S.; Duman, S.; Dede, Y.; Dolen, Y.; Kilic, B.; Kostereli, Z.; Yildirim, L. T.; Dogan, A. L.; Guc, D.; et al. Designing Excited States: Theory-Guided Access to Efficient Photosensitizers for Photodynamic Action. *Angew. Chem.* **2011**, *123*, 12143–12147.
- (51) Pang, W.; Zhang, X.-F.; Zhou, J.; Yu, C.; Hao, E.; Jiao, L. Modulating the Singlet Oxygen Generation Property of Meso–B Directly Linked BODIPY Dimers. *Chem. Commun.* **2012**, *48*, 5437–5439.
- (52) Wu, W.; Cui, X.; Zhao, J. Hetero BODIPY-Dimers as Heavy Atom-Free Triplet Photosensitizers Showing a Long-Lived Triplet Excited State for Triplet—Triplet Annihilation Upconversion. *Chem. Commun.* **2013**, *49*, 9009—9011.
- (53) Alamiry, M. A.; Bahaidarah, E.; Harriman, A.; Olivier, J.-H.; Ziessel, R. Influence of Applied Pressure on the Probability of Electronic Energy Transfer Across A Molecular Dyad. *Pure Appl. Chem.* **2013**, *85*, 1349–1365.
- (54) Kolemen, S.; Bozdemir, O. A.; Cakmak, Y.; Barin, G.; Erten-Ela, S.; Marszalek, M.; Yum, J.-H.; Zakeeruddin, S. M.; Nazeeruddin, M. K.; Grätzel, M.; et al. Optimization Of Distyryl- BODIPY Chromophores For Efficient Panchromatic Sensitization In Dye Sensitized Solar Cells. *Chem. Sci.* **2011**, *2*, 949–954.
- (55) Savoldelli, A.; Paolesse, R.; Fronczek, F. R.; Smith, K. M.; Vicente, M. G. H. BODIPY Dyads from A, C-Biladiene Salts. *Org. Biomol. Chem.* **2017**, *15*, 7255–7257.
- (56) Senge, M. O.; Gerzevske, K. R.; Vicente, M. G. H.; Forsyth, T. P.; Smith, K. M. Models for the Photosynthetic Reaction Center—Synthesis and Structure of Porphyrin Dimers with Cis-and Trans-Ethene and Skewed Hydroxymethylene Bridges. *Angew. Chem., Int. Ed. Engl.* 1993, 32, 750–753.
- (57) Jaquinod, L.; Nurco, D. J.; Medforth, C. J.; Pandey, R. K.; Forsyth, T. P.; Olmstead, M. M.; Smith, K. M. Synthesis and Characterization of Bis (chlorin) s from the Mcmurry Reaction of Formylchlorins. *Angew. Chem., Int. Ed. Engl.* **1996**, *35*, 1013–1016.
- (58) Locos, O.; Bašić, B.; McMurtrie, J. C.; Jensen, P.; Arnold, D. P. Homo- and Heteronuclear Meso, Meso-(E)-Ethene-1, 2-Diyl-Linked Diporphyrins: Preparation, X-Ray Crystal Structure, Electronic Absorption and Emission Spectra and Density Functional Theory Calculations. *Chem. Eur. J.* 2012, 18, 5574–5588.
- (59) Peña-Cabrera, E.; Aguilar-Aguilar, A.; González-Domínguez, M.; Lager, E.; Zamudio-Vázquez, R.; Godoy-Vargas, J.; Villanueva-García, F. Simple, General, and Efficient Synthesis of Meso-Substituted Borondipyrromethenes from a Single Platform. *Org. Lett.* 2007, *9*, 3985–3988.
- (60) Ahrens, J.; Haberlag, B.; Scheja, A.; Tamm, M.; Bröring, M. Conjugated BODIPY Dyemers by Metathesis Reactions. *Chem. Eur. J.* 2014, 20, 2901–2912.
- (61) Saiyed, A. S.; Patel, K. N.; Kamath, B. V.; Bedekar, A. V. Synthesis of Stilbene Analogues by One-Pot Oxidation-Wittig and Oxidation-Wittig-Heck Reaction. *Tetrahedron Lett.* **2012**, *53*, 4692–4696
- (62) Kancharla, P.; Reynolds, K. A. Synthesis of 2, 2'-Bipyrrole-5-Carboxaldehydes and Their Application in the Synthesis of B-Ring Functionalized Prodiginines and Tambjamines. *Tetrahedron* **2013**, *69*, 8375–8385.

- (63) Bosanac, T.; Wilcox, C. S. Precipiton Reagents: Precipiton Phosphines for Solution-Phase Reductions. *Org. Lett.* **2004**, *6*, 2321–2324.
- (64) Park, K.; Bae, G.; Moon, J.; Choe, J.; Song, K. H.; Lee, S. Synthesis of Symmetrical and Unsymmetrical Diarylalkynes from Propiolic Acid Using Palladium-Catalyzed Decarboxylative Coupling. *J. Org. Chem.* **2010**, *75*, 6244–6251.
- (65) McMurry, J. E. Carbonyl-Coupling Reactions Using Low-Valent Titanium. Chem. Rev. 1989, 89, 1513–1524.
- (66) Garrido Montalban, A.; Herrera, A. J.; Johannsen, J.; White, A. J.; Williams, D. J. Phenanthroline–Dipyrromethene Conjugates: Synthesis, Characterization, and Spectroscopic Investigations. *Tetrahedron* 2014, 70, 7358–7362.
- (67) Li, T.; Gu, W.; Yu, C.; Lv, X.; Wang, H.; Hao, E.; Jiao, L. Syntheses and Photophysical Properties Of Meso-Phenylene Bridged Boron Dipyrromethene Monomers, Dimers and Trimer. *Chin. J. Chem.* **2016**, 34, 989–996.
- (68) Kasha, M. Energy Transfer Mechanisms and the Molecular Exciton Model for Molecular Aggregates. *Radiat. Res.* **1963**, *20*, 55–70
- (69) Whited, M. T.; Patel, N. M.; Roberts, S. T.; Allen, K.; Djurovich, P. I.; Bradforth, S. E.; Thompson, M. E. Symmetry-Breaking Intramolecular Charge Transfer in the Excited State of Meso-Linked BODIPY Dyads. *Chem. Commun.* **2012**, *48*, 284–286.
- (70) Yanai, T.; Tew, D.; Handy, N. A New Hybrid Exchange—Correlation Functional Using the Coulomb-Attenuating Method (CAM-B3LYP). *Chem. Phys. Lett.* **2004**, 393, 51–57.
- (71) Zhao, Y.; Truhlar, D. G. The M06 Suite of Density Functionals for Main Group Thermochemistry, Thermochemical Kinetics, Noncovalent Interactions, Excited States, and Transition Elements: Two New Functionals and Systematic Testing of Four M06-Class Functionals and 12 Other Functionals. *Theor. Chem. Acc.* 2008, 120, 215–241.
- (72) Bauernschmitt, R.; Ahlrichs, R. Treatment of Electronic Excitations Within the Adiabatic Approximation of Time Dependent Density Functional Theory. *Chem. Phys. Lett.* **1996**, 256, 454–464.
- (73) Laurent, A. D.; Adamo, C.; Jacquemin, D. Dye Chemistry with Time-Dependent Density Functional Theory. *Phys. Chem. Chem. Phys.* **2014**, *16*, 14334–14356.
- (74) Le Guennic, B.; Jacquemin, D. Taking up the Cyanine Challenge with Quantum Tools. *Acc. Chem. Res.* **2015**, *48*, 530–537. (75) Adamo, C.; Jacquemin, D. The Calculations of Excited-State Properties with Time-Dependent Density Functional Theory. *Chem. Soc. Rev.* **2013**, *42*, 845–856.
- (76) Miertuš, S.; Scrocco, E.; Tomasi, J. Electrostatic Interaction of a Solute with a Continuum. A Direct Utilizaion of AB Initio Molecular Potentials for the Prevision of Solvent Effects. *Chem. Phys.* **1981**, *55*, 117–129.
- (77) Tomasi, J.; Mennucci, B.; Cammi, R. Quantum Mechanical Continuum Solvation Models. *Chem. Rev.* **2005**, *105*, 2999–3094.
- (78) Frisch, M. J.; Trucks, G. W.; Schlegel, H. B.; Scuseria, G. E.; Robb, M. A.; Cheeseman, J. R.; Scalmani, G.; Barone, V.; Mennucci, B.; Petersson, G. A.; et al. *Gaussian 09*, Revision A.02; Gaussian, Inc.: Wallingford, CT, 2009.